

Final state interactions in pion production from nuclei

M. Alqadi and W. R. Gibbs

Department of Physics, New Mexico State University, Las Cruces, New Mexico 88003

(Received 16 August 2002; published 6 December 2002)

We have calculated the effect of the inclusion of final state interactions on pion production from nuclei with incident pion beams. We find that the effect of absorption, along with geometric considerations, explains much of the enhancement at low invariant mass seen in recent data for invariant-mass spectra with increasing atomic number. While the variation among nuclei is well reproduced for all charge states, the enhancement for the ratio for heavy nuclei to deuterium for the $\pi^+\pi^-$ final state is only partially understood.

DOI: 10.1103/PhysRevC.66.064604

PACS number(s): 25.80.Hp, 13.75.Gx

I. INTRODUCTION

The pion induced pion production on both a free nucleon and a nucleon within nuclear material provides an opportunity to study the mechanism for pion production. In a series of papers [1–5] the results of experiments done at the CHAOS (Canadian High Acceptance Orbit Spectrometer) at TRIUMF were presented on pion production with pion beams for several nuclei. Specifically, the collaboration reported data for the $\pi^+A \rightarrow \pi^+\pi^-X$ and $\pi^+A \rightarrow \pi^+\pi^+X$ reactions on ${}^2\text{H}$, ${}^{12}\text{C}$, ${}^{40}\text{Ca}$ and ${}^{208}\text{Pb}$ at an incident pion kinetic energy of 283 MeV. The results showed that the shape of the invariant-mass distribution of the two final pions changes with atomic mass number.

An examination of the changes among the heavy nuclei (carbon and heavier) reveals that the variation is about the same for the two final charge states. The shape of the spectrum for the case of a deuteron target is very different for the two cases.

A striking feature of the raw spectra is a large peak at small invariant mass of the two-pion system. This peak is at least partly the result of the experimental conditions and can be regarded as a Jacobian peak related to the acceptance of the spectrometer. Since the correction for this large instrumental effect is difficult to make, the results are often presented as ratios, in the expectation that the acceptance effect will cancel. Thus, Ref. [3] gives ratios to the deuteron cross section, a common way to normalize. However, in this case, since the deuteron results are very different for the two final charge states, this procedure results in very different spectral ratios for them. If one instead takes ratios to the carbon cross sections, the calcium and lead results are about the same for the two final charge states.

Shortly after these first data, experiments [6] done by the Crystal Ball Collaboration at Brookhaven National Laboratory produced data on the production of two neutral pions for D, C, Al, and Cu with a negative pion beam. One sees a very similar trend for the ratios in these data to that of the CHAOS data.

Since the basic conclusion of these data sets is that the heavier the nucleus, the more the invariant-mass spectrum is peaked toward lower values of invariant mass, a number of groups have seen in this data possible evidence for a supposed modification of the $\pi\pi$ interaction in nuclear matter. In early work, a theoretical expectation of an enhancement of

strength in the $\pi^+\pi^-$ channel for $I=J=0$ near the threshold was suggested by Schuck *et al.* [7] based on an analogy with Cooper pairs.

Recently, several studies have placed emphasis on medium effects to explain the strength enhancement of $M_{\pi\pi}$ distribution in the $\pi^+\pi^-$ channel (σ -meson channel). The calculation of Rapp *et al.* [8] is based on a simple model in which the pion production takes place as an elementary reaction. In their model two contributions were included, a single pion exchange reaction and the excitation followed by the decay of the $N^*(1440)$ into two pions and a nucleon. The $\pi\pi$ final state interaction is included by using the chirally improved Jülich model [9] and several medium effects were included. There is reasonable agreement of their calculation and the CHAOS data in both the $\pi^+\pi^-$ and $\pi^+\pi^+$ channels.

Vicente-Vacas and Oset [10] used a microscopic model for the pion production with final state interaction among the pions included in the nuclear medium. Several nuclear effects were taken into account in their study including an approximate treatment of pion absorption, Pauli blocking, and Fermi motion. Their calculation reproduced the CHAOS data for calcium in the $\pi^+\pi^+$ channel reasonably well and also gave a reasonable agreement for the deuteron. In contrast, this model failed to reproduce the CHAOS data in the $\pi^+\pi^-$ channel except for ${}^2\text{H}$.

The enhancement of strength in the $I=J=0$ channel $\pi^+\pi^-$ channel near the threshold was argued by Hatsuda *et al.* [11] to be due to the partial restoration of chiral symmetry in nuclear matter. Davesne *et al.* [12] included the effect of chiral symmetry restoration and the influence of collective nuclear pionic modes and found an enhancement of the spectral function to be a small energy. Aouissat *et al.* [13] argued that the combination of effects of the restoration of chiral symmetry [11] in nuclear matter and standard many body correlation could explain the strength of the spectrum $M_{\pi\pi}$ near threshold [7].

While these considerations may be correct there may also be more prosaic reasons for the increasing strength at low invariant mass. We investigate the effect of the final state interaction of the two individual pions with the nucleus, especially the absorption of the pion. Our calculation contains no free parameters and pays special attention to the geometry of the reaction.

We make two simplifying assumptions.

(i) The energy of the recoiling nucleons is neglected. This can be justified, to some extent, because the nucleus carries off the remaining energy and momentum as a single entity to the extent that it stays together. This is true for $A-1$ of the nucleons [2] and the single nucleon can still be co-moving with the $A-1$. Since the nucleons are much heavier than the pions, they can carry a large amount of momentum with a negligible amount of energy. In this extreme case the total beam energy is passed on to the two-pion system. The alternative to this assumption would be a considerably more complicated calculation, perhaps warranted but beyond the scope of the present work. The invariant mass of the two-pion system is given by

$$M = 2\sqrt{\mu^2 + q^2}, \quad (1)$$

where μ is the pion mass (charged or neutral as appropriate) and \mathbf{q} is the momentum of one of the pions in the two-pion rest frame, the internal momentum. The above assumption then leads to the relation

$$\omega = \sqrt{M^2 + Q^2}, \quad (2)$$

where ω is the initial beam energy and \mathbf{Q} is the total momentum of the two-pion pair. This assumption will lead to some overestimate of the energy carried by the pion pair changing the shape of the spectrum of produced pions. The most significant difference can be expected at high invariant masses. We restrict the present study to the lower half of the spectrum where we have verified that the shape of the production spectrum makes a negligible difference to the ratios.

(ii) We assume that the production takes place at a fixed point on the surface of the nucleus in a plane at the equator perpendicular to the beam direction. The reaction probability is greatly enhanced in this region for two reasons. First, there is a simple geometrical factor of the distance to the center of the nucleus. Second, if the incident pion comes in with a small impact parameter either the initial pion will be scattered (even a moderate loss of energy will make the pion production impossible) or one of the final pions will very likely be absorbed, having to pass through the entire nucleus to escape. Thus, the reactions in which the incident pion has a small impact parameter are greatly suppressed. This point is discussed in Ref. [10].

II. TECHNIQUE

A. Qualitative overview

It is possible to see in a simple qualitative manner that pion absorption in the final state will lead to a relative enhancement of the invariant-mass spectrum at low pion invariant masses. For a first orientation we will assume that the pion pair proceeds forward in the direction of the initial beam since the distribution of the momentum of the pair is expected to be very forward peaked. For the purposes of the diagram only (see Fig. 1) we also take the momentum of one pion in the frame of the two-pion system, \mathbf{q} , to be perpendicular to the beam direction.

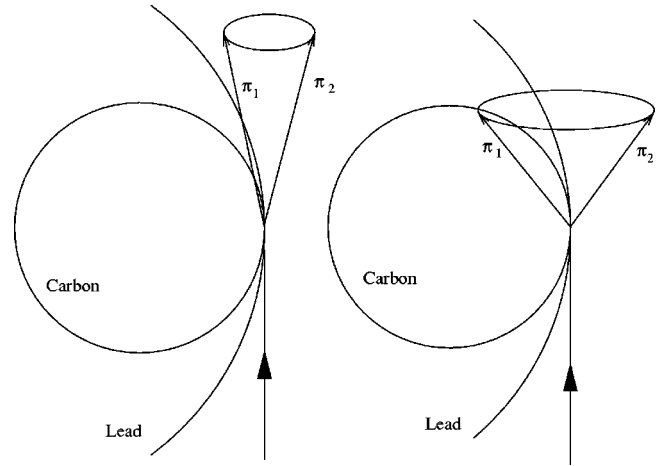


FIG. 1. Schematic view of the basic effect.

With these simplifying assumptions we may now consider the effect of the absorption of the pions in the final state on the shape of the invariant-mass spectrum. Figure 1 shows two cases. The left portion of the sketch corresponds to the situation where the invariant mass is small, so the internal momentum is small and the momentum of the total two-pion system is large, leading to a narrow cone representing the paths of the two pions. It is seen that the pions are exposed to relatively little interaction with nuclear matter. In the limit of the internal momentum becoming zero, the pions would encounter no higher nuclear density than that in which they were formed. In this limit the size of the nucleus would matter very little.

In the right portion of the diagram a case is illustrated in which the invariant mass and internal momentum are larger. In this case it is seen that a large fraction of the pions must traverse a significant amount of nuclear matter. The larger the nucleus, the larger the probability that one member of the pion pair would get absorbed. Hence, we can anticipate that the geometry of the absorption in the final state leads to a depletion of the higher values of the invariant-mass spectrum and that the effect becomes more important with increasing A .

B. Calculation

The method used here is very similar to that of Oset and Vicente Vacas [14]. However, they calculated the effect only for calcium and used an eikonal approximation for the propagation of the final pions.

We assume that the pion pair is formed quickly at short range by the strong interaction, and that this formation is independent of the nucleus that it is near. Also, we assume that the final total momentum of the two pions is in the same direction as the incident beam. This assumption of exact forward propagation of the pair was investigated by calculating with finite angles. It was found that the dependence on this angle was very small. We define the spherical angles θ and ϕ from the beam axis as the direction of the π^+ in the center of the mass of the pair.

After formation the pions are allowed to propagate independently in Coulomb and strong nuclear potentials with

relativistic motion. Their momenta and coordinates are propagated with the equations

$$\mathbf{p}(t + \delta t) = \mathbf{p}(t) + \mathbf{F} \delta t \quad (3)$$

and

$$\mathbf{r}(t + \delta t) = \mathbf{r}(t) + \frac{\mathbf{p}(t)}{E(t)} \delta t, \quad (4)$$

where \mathbf{F} is the resultant of the Coulomb and strong interaction forces. We take the electric charge distribution of the nucleus to be

$$\rho_c(r) = \frac{\rho_0}{1 + e^{r - \gamma/\alpha}}. \quad (5)$$

The values of γ and α were taken from Ref. [15] and are (in fm) (2.44, 0.5), (3.07, 0.519), (3.65, 0.54), (4.252, 0.589), and (6.6, 0.55) for C, Al, Ca, Cu, and Pb, respectively. The constant ρ_0 was fixed by normalizing the integral of the density to the total charge Ze .

The nuclear potential is given by

$$V_s(r) = -\frac{2\pi}{mA}(Nf_{\pi n} + Zf_{\pi p})\rho(r), \quad (6)$$

where N, Z are the number of neutrons and protons and A is the atomic mass number. $\rho(r)$ is the nuclear strong density, i.e., the density of the centers of the nucleons,

$$\rho(r) = \frac{\rho_0}{1 + e^{r - c/a}}. \quad (7)$$

The values of c and a were (2.25, 0.5), (2.95, 0.5), (3.55, 0.54), (4.23, 0.55) and (6.5, 0.55), for C, Al, Ca, Cu, and Pb, respectively, and $f_{\pi n}$ and $f_{\pi p}$ are the real parts of the forward amplitudes of the πn and πp amplitudes [16]. This real potential is modeled after the pion-nucleus optical potential. We will see later that these nonabsorptive strong interactions play a minor role in the result.

For each initial value of the invariant mass (M_i) we calculate the internal momentum, the total momentum of the two-pion pair, and, with values of the angles of these two quantities, the initial values of the momenta for each pion can be determined. The pions are then propagated to a large distance (into free space) and a new invariant mass is calculated for the pair (M_f). In this way the function

$$M_f(x, \phi, M_i), \quad (8)$$

where $x = \cos \theta$, is established. It depends on the angles of both \mathbf{q} and \mathbf{Q} but we suppress the dependence on the angles of \mathbf{Q} .

The final spectrum (without absorption) will be given by

$$S_f(x, \phi, M_f) = \frac{d\sigma}{dM_f} = \frac{d\sigma}{dM_i} \left/ \frac{dM_f}{dM_i} \right. = S_i(x, \phi, M_i) \left/ \frac{dM_f}{dM_i} \right. \quad (9)$$

Because the derivative in the denominator is sometimes zero, sharp peaks appear in the spectra for individual values of the momentum directions. The integration over the angles results in a smooth spectrum but, since the integration is done numerically, some care is required to obtain a presentable curve. The lines shown in the figures have been smoothed since the final calculated values still show a small residual ripple. We use as a simple model for the initial spectrum two body phase space.

C. Absorption factor

Pion absorption is an important factor during the passage of pions through the residual nucleus. It reduces the cross section for pion production and affects the shape of the spectrum. We include the effects of absorption by calculating the factor of the probability that the pion has not been absorbed, $P(\mathbf{r})$, at the point \mathbf{r} as follows. The probability of survival is given by

$$P(\mathbf{r}) = 1 - \int_{\mathbf{r}_0}^{\mathbf{r}} \lambda(\mathbf{r}') P(\mathbf{r}') d\mathbf{l}, \quad (10)$$

where \mathbf{r}_0 is the formation point, and the initial value of $P \equiv 1$. The integral is taken along the trajectory of the particle. The probability of survival can also be written as

$$P(\mathbf{r}) = \exp\left(-\int_{\mathbf{r}_0}^{\mathbf{r}} \lambda(\mathbf{r}') d\mathbf{l}\right). \quad (11)$$

As in Ref. [14], the absorption probability per unit length is assumed to be proportional to the square of the nuclear density

$$\lambda(r) = \lambda_0(E) \rho^2(r). \quad (12)$$

The λ_0 parameter depends on the energy of the pion and is obtained by fitting to absorption data. For light nuclei we first calculated the eikonal expression for the total absorption cross section,

$$\sigma(\lambda_0) = 2\pi \int_0^\infty a da \left[1 - \exp\left(-\int_{-\infty}^\infty dz \lambda_0 \rho^2(\sqrt{z^2 + a^2})\right) \right]. \quad (13)$$

By comparing the values of $\sigma(\lambda_0)$ with experimental values of $\sigma_{abs}(E)$ [17–22] we inferred the values of $\lambda_0(E)$ needed to fit the data (see Fig. 2). We found that the values of $\lambda_0(E)$ had little dependence on the atomic mass number A for light nuclei.

For the case of calcium we compared calculations using the Woods-Saxon density and a shell model density for calcium [23]. The difference was scarcely visible on a plot.

For heavy nuclei it is important to follow the trajectory instead of using Eq. (13). Figure 3 shows the result of the fit for gold. The λ_0 used in this case is also given in Fig. 2. It is unfortunate that the λ_0 's determined in these two regions of A are so different. There are possible physics reasons that they are different but the data fits are from different groups and use different techniques as well. Only values below about 100 MeV are important for our results.

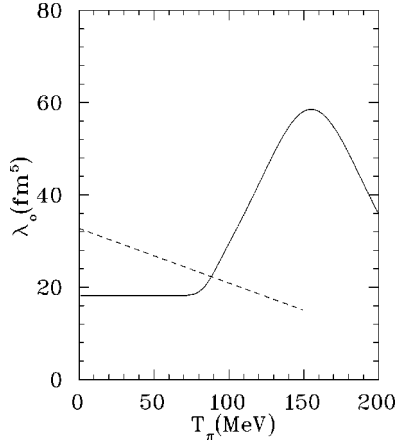


FIG. 2. λ_0 determined for light nuclei (solid curve) and for gold (dashed curve).

Denoting the result of following the trajectory of the i th pion into free space by $P_i(x, \phi, M_i)$ the final spectrum is given by the integral over all possible decay angles,

$$S_f(M_f) = \frac{1}{4\pi} \int_{-1}^1 dx \int_0^{2\pi} d\phi S_f(x, \phi, M_f) \times P_1(x, \phi, M_i) P_2(x, \phi, M_i). \quad (14)$$

III. RESULTS

Figure 4 shows the resulting spectra as well as the original model spectrum (solid line). Also shown is the spectrum with only the strong and Coulomb potentials. These spectra cannot easily be compared directly to the data for two reasons.

(i) Our initial model spectrum represents only roughly the free spectrum for $\pi^+\pi^+$ and does not represent well the spectrum for $\pi^+\pi^-$. In fact, the free spectrum is not well known. Even if it were, we cannot be sure that it is the appropriate starting spectrum in the nuclear case.

(ii) There is a large instrumental acceptance correction to be made.

For these reasons we, like the experimental group, com-

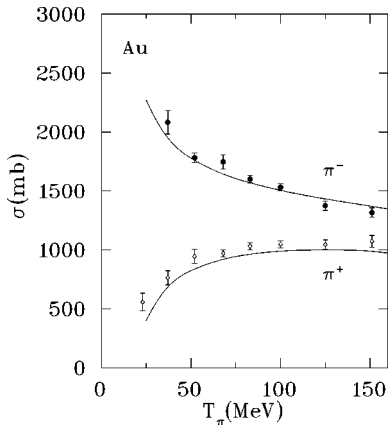


FIG. 3. Comparison of the absorption cross section computed with the dashed curve in Fig. 2 with the absorption data of Nakai *et al.* (Ref. [18]).

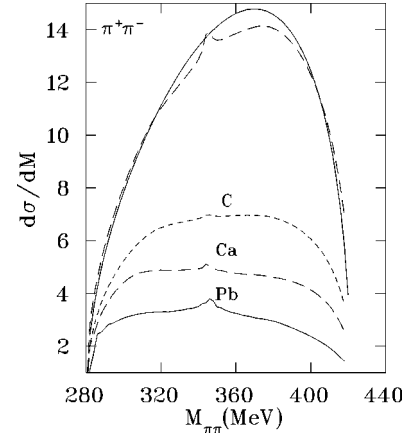


FIG. 4. Variation of the basic spectrum for carbon, calcium, and lead. The solid curve shows the shape the initial free spectrum and the long-dashed curve represents the modification due to the non-absorptive interactions only.

pare with ratios. Since we are interested in the increase of the spectrum ratios near small values of invariant mass we normalize the ratios (theoretical and experimental) to unity at 330 MeV.

The CHAOS group calculated the ratio $A S_{\pi\pi} / D S_{\pi\pi}$ for both $\pi^+\pi^-$ and $\pi^+\pi^+$ to show the effect of the nucleus. The strong enhancement near threshold is due to the fact that the invariant-mass distribution of D (^2H) and A (^{12}C , ^{40}Ca , ^{208}Pb) change dramatically near the threshold where is a much smaller peak in the D distribution. In our study we calculated the ratio of heavier nuclei to carbon instead of deuterium and found that the ratio increases with A for all charge channels by almost the same amount.

Figures 5 and 6 show the ratios of the cross sections for ^{208}Pb and ^{40}Ca to that of ^{12}C . The calculated ratios are seen to reproduce the experimental data in the $\pi^+\pi^+$ and $\pi^+\pi^-$ channels. The two charge channels show similar behavior.

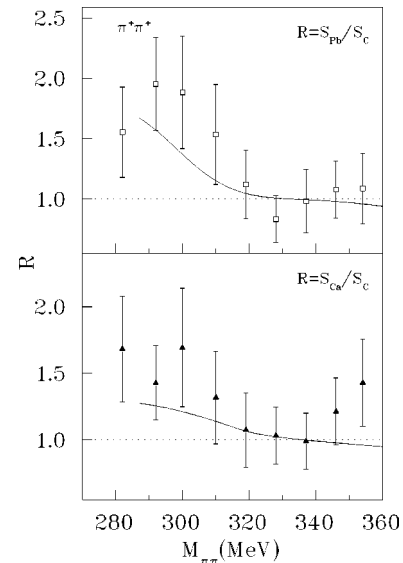


FIG. 5. Ratios for lead and calcium to carbon for the $\pi^+\pi^+$ final state compared with the CHAOS data (Ref. [3]).

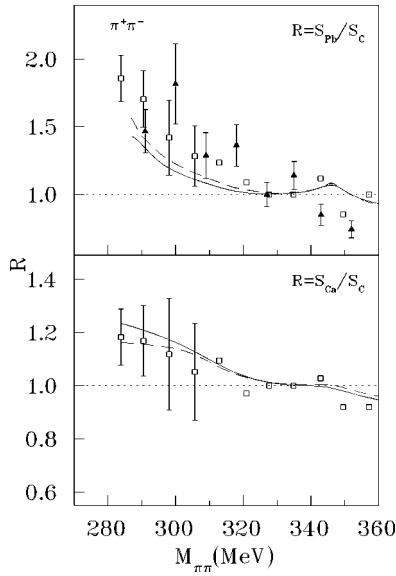


FIG. 6. Ratios for the $\pi^+\pi^-$ final state compared with the CHAOS data (Ref. [3]) (squares) and (Ref. [1]) (triangles). The solid line is the result of a calculation with $r=c$ and the dashed line was made with $r=c+a$.

Figure 6 also shows the effect of varying the assumed radius at which the production takes place.

Figure 7 shows the difference seen in the lead to carbon ratio using the value of λ_0 determined from the gold data and that obtained from the light element fit. Figure 8 shows the dependence on the final charge state of the calculations. It is seen that the effect is moderate.

Figure 9 shows the ratio of the cross sections for Cu and Al to C compared to the experimental data in the $\pi^0\pi^0$ channel. Although the error bars are large, the trend of the data is clearly reproduced.

The estimate of the interaction potential to use in a classical calculation by a quantum model must, of course, be approximate. Figure 10 shows that this potential plays a minor role by comparing with calculations with it set to zero.

Figure 11 shows the ratios of the heavy elements to deu-

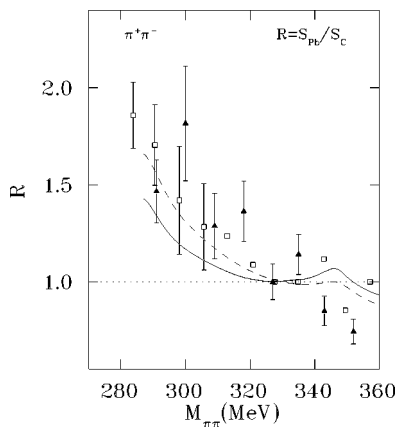


FIG. 7. Comparison of the ratio calculated using values of λ_0 obtained from the fit to gold (solid) and the light nuclei (dashed). The data is the same as in Fig. 6.

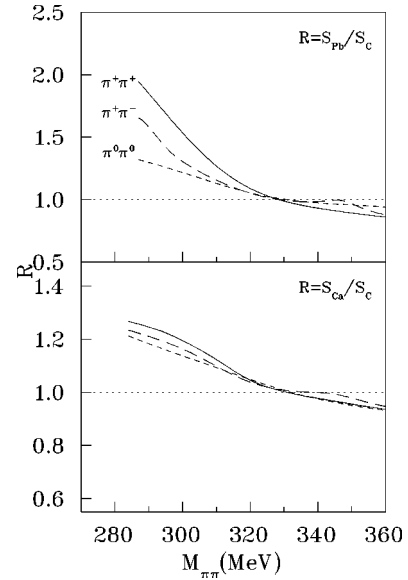


FIG. 8. Comparison of results for different charge states for the lead to carbon ratio. The solid curve corresponds to the $\pi^+\pi^+$ final state, the short dash to the neutral final state, and the long dash to the $\pi^+\pi^-$ final state.

terium for the $\pi^+\pi^+$ final state. The comparison between theory and experiment is satisfactory.

Figure 12 shows the ratio of the lead spectrum to that of deuterium for the $\pi^+\pi^-$ final state. The effect considered here is able to explain only a little less than half of the observed experimental effect.

IV. DISCUSSION

We have seen that the variation in the spectral shape from nucleus to nucleus (above deuterium) can be understood in terms of the interaction of the produced pions with the

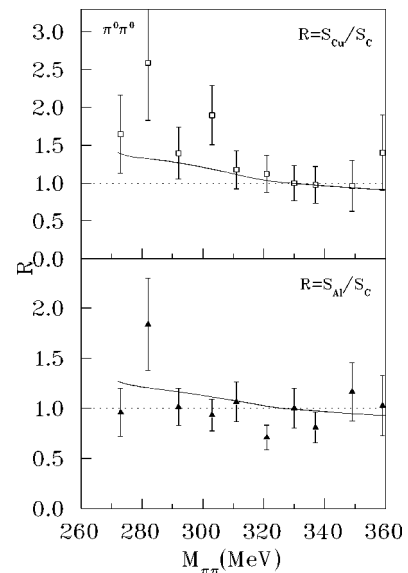


FIG. 9. Results for the ratios for the $\pi^0\pi^0$ final state compared with the Crystal Ball data (Ref. [6]).

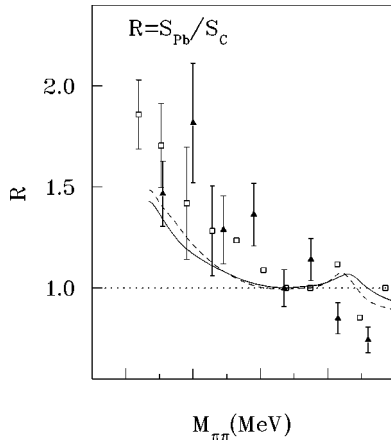


FIG. 10. Results showing the effect of setting the strong potential to zero for the $\pi^+\pi^-$ final state. The solid curve is calculated with the strong potential and the dashed curve has it set to zero.

nucleus. The size of the nucleus plays a strong role in this explanation. Thus, there is little or no evidence in these ratios for a modification of the pion production or pion-pion interaction. It is not clear that one should expect an effect of this type in any case. As has been discussed, the point at which the production takes place is largely determined by the density. Thus, as one moves to heavier nuclei there will be a strong tendency for the reaction to occur at the same density. Since the average density is the major parameter used to determine the medium effect, and it tends to remain constant, one might believe that no nuclear matter effect on the production would be seen in comparing among heavy nuclei.

Having said that, one must admit that there is some variation in the expected density going from (say) carbon to lead. If we use the linear dependence of the condensate on the density of Cohen, Furnstahl, and Griegel [24] with the calculation of the change in the shape of the spectrum by

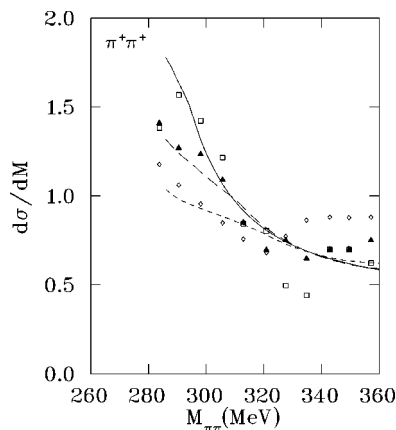


FIG. 11. Ratios of the spectra of heavy nuclei divided by the basic spectrum for the $\pi^+\pi^+$ final state. The squares and solid curve correspond to lead, the triangles and long-dashed curve to calcium, and the diamonds and short-dashed curve to carbon.

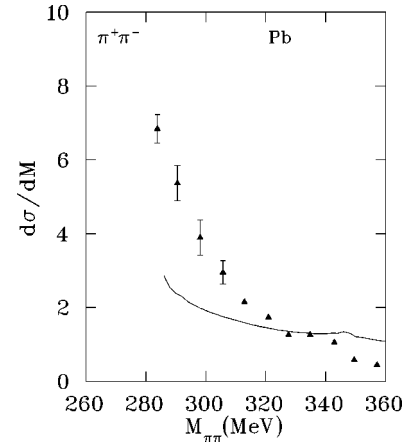


FIG. 12. Ratio of the lead spectrum to the basic spectrum for the $\pi^+\pi^-$ final state.

Hatsuda and collaborators [11] along with a guess of the change in nuclear density, the result is of the same order as the discrepancy seen in the upper part of Fig. 6 or in Fig. 10. However, one must be very careful about trying to draw any conclusion from this since this is also about the same order as the difference between the two choices in λ_0 as seen in Fig. 7, and not far outside experimental errors.

Of course, one might try to compare the production on the nucleon with production in the nucleus which is close to what has been done before. One would have to assume that the mechanism was simply production from one of the nucleons in the nucleus [2]. In the present experiments the comparison has been made with the deuteron.

It has long been known (see Ref. [22], for example) that the shape of the invariant-mass spectrum for the $\pi^+\pi^-$ final pair is different from that of the $\pi^+\pi^+$ pair at low incident energy. According to Ref. [10] the sharp decrease in the low mass region is due to a cancellation in diagrammatic contributions. These authors suggest that an alteration of the cancellation due to interaction with the surrounding nucleons might lead to a modification in this cancellation and thus to a change in shape of the production spectrum in the direction seen.

It is also clear (see again Ref. [22]) that the $\pi^+\pi^-$ spectrum shape changes to more closely resemble the $\pi^+\pi^+$ distribution (and phase space) as the energy increases. As one goes from the reaction on a single nucleon to that on a nucleus the effective energy at which the reaction takes place becomes higher due to the possibilities of coherent production. Thus, one should also expect an increase of strength in the low mass part of the spectrum from this effect as well.

ACKNOWLEDGMENTS

This work was supported by the National Science Foundation (Grant No. 0099729) and the Jordan University of Science and Technology.

- [1] F. Bonutti, P. Camerini, E. Fragiaco, N. Grion, R. Rui, P. A. Amaudruz, J. T. Brack, L. Felawka, E. F. Gibson, G. J. Hofman, M. Kermani, E. L. Mathie, S. McFarland, R. Meier, D. Ottewell, K. Raywood, M. E. Sevier, G. R. Smith, and R. Tacik, *Phys. Rev. Lett.* **77**, 603 (1996).
- [2] F. Bonutti, P. Camerini, E. Fragiaco, N. Grion, R. Rui, J. T. Brack, L. Felawka, E. F. Gibson, G. Hofman, M. Kermani, E. L. Mathie, S. McFarland, R. Meier, D. Ottewell, K. Raywood, M. E. Sevier, G. R. Smith, R. Tacik, and The CHAOS Collaboration, *Phys. Rev. C* **55**, 2998 (1997).
- [3] F. Bonutti, P. Camerini, E. Fragiaco, N. Grion, R. Rui, J. T. Brack, L. Felawka, E. F. Gibson, G. Hofman, M. Kermani, E. L. Mathie, S. McFarland, R. Meier, K. Raywood, D. Ottewell, M. E. Sevier, G. R. Smith, R. Tacik, and The CHAOS Collaboration, *Phys. Rev. C* **60**, 018201 (1999).
- [4] F. Bonutti *et al.*, *Nucl. Phys.* **A677**, 213 (2000).
- [5] P. Camerini, E. Fragiaco, N. Grion, R. Rui, J. T. Brack, E. F. Gibson, G. J. Hofman, E. L. Mathie, R. Meier, K. Raywood, M. E. Sevier, G. R. Smith, and R. Tacik, *Phys. Rev. C* **64**, 067601 (2001).
- [6] A. Starostin *et al.*, The Crystal Ball Collaboration, *Phys. Rev. Lett.* **85**, 5539 (2000).
- [7] P. Schuck *et al.*, *Z. Phys.* **330**, 119 (1988).
- [8] R. Rapp, J. W. Durso, Z. Aouissat, G. Chanfray, O. Krehl, P. Schuck, J. Speth, and J. Wambach, *Phys. Rev. C* **59**, R1237 (1999).
- [9] R. Rapp, J. W. Durso, and J. Wambach, *Nucl. Phys.* **A596**, 436 (1996); D. Lohse, J. W. Durso, K. Holinde, and J. Speth, *Phys. Lett. B* **234**, 235 (1989); *Nucl. Phys.* **A516**, 513 (1990).
- [10] M. J. Vicente-Vacas and E. Oset, *Phys. Rev. C* **60**, 064621 (1999).
- [11] T. Hatsuda, T. Kunihiro, and G. Chanfray, *Phys. Rev. Lett.* **82**, 2840 (1999); D. Jido, T. Hatsuda, and T. Kunihiro, *Phys. Rev. D* **63**, 011901 (2001).
- [12] D. Davesne, Y. J. Zhang, and G. Chanfray, *Phys. Rev. C* **62**, 024604 (2000).
- [13] Z. Aouissat, G. Chanfray, P. Schuck, and J. Wambach, *Phys. Rev. C* **61**, 012202 (2000).
- [14] E. Oset and M. J. Vicente Vacas, *Nucl. Phys.* **A446**, 584 (1985).
- [15] H. De Vries *et al.*, *At. Data Nucl. Data Tables* **36**, 496 (1987).
- [16] See the VPI/GWU phase-shift analysis, available on the internet at <http://gwdac.phys.gwu.edu/>
- [17] D. Ashery *et al.*, *Phys. Rev. C* **23**, 2173 (1981).
- [18] K. Nakai *et al.*, *Phys. Rev. Lett.* **44**, 1446 (1980).
- [19] R. Salukvadze and D. Neagu, *Zh. Éksp. Teor. Fiz.* **41**, 78 (1961) [*Sov. Phys. JETP* **14**, 59 (1962)].
- [20] M. P. Balandin, O. Ivanov, V. Moiseenko, and G. Sokolov, *Zh. Éksp. Teor. Fiz.* **46** 415 (1964) [*Sov. Phys. JETP* **19**, 279 (1964)].
- [21] J. V. Laberrigue-Frolova, M. P. Balandin, and S. Z. Otvinoskii, *Zh. Éksp. Teor. Fiz.* **37**, 634 (1960) [*Sov. Phys. JETP* **10**, 452 (1960)].
- [22] J. Kirz, J. Schwartz, and R. D. Tripp, *Phys. Rev.* **130**, 2481 (1963).
- [23] W. R. Gibbs and J-P. Dedonder, *Phys. Rev. C* **46**, 1825 (1992).
- [24] T. D. Cohen, R. J. Furnstahl, and D. K. Griegel, *Phys. Rev. C* **45**, 1881 (1992).